General Disclaimer

One or more of the Following Statements may affect this Document

- This document has been reproduced from the best copy furnished by the organizational source. It is being released in the interest of making available as much information as possible.

- This document may contain data, which exceeds the sheet parameters. It was furnished in this condition by the organizational source and is the best copy available.

- This document may contain tone-on-tone or color graphs, charts and/or pictures, which have been reproduced in black and white.

- This document is paginated as submitted by the original source.

- Portions of this document are not fully legible due to the historical nature of some of the material. However, it is the best reproduction available from the original submission.

Produced by the NASA Center for Aerospace Information (CASI)

DEPARTMENT OF PHYSICS
SCHOOL OF SCIENCES AND HEALTH PROFESSIONS
OLD DOMINION UNIVERSITY
NORFOLK, VIRGINIA

Technical Report PTR 83-1

THEORETICAL STUDIES OF SOLAR-PUMPED LASERS

By

Wynford L. Harries, Principal Investigator

Progress Report
For the period July 16, 1982 to January 15, 1983

FEB 1983
RECEIVED
NASA STI FACIL...

January 1983

DEPARTMENT OF PHYSICS
SCHOOL OF SCIENCES AND HEALTH PROFESSIONS
OLD DOMINION UNIVERSITY
NORFOLK, VIRGINIA

Technical Report PTR 83-1

THEORETICAL STUDIES OF SOLAR-PUMPED LASERS

By

Wynford L. Harries, Principal Investigator

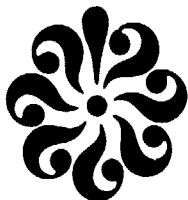

Progress Report
For the period July 16, 1982 to January 15, 1983

Prepared for the
National Aeronautics and Space Administration
Langley Research Center
Hampton, Virginia 23665

Under
Research Grant NSG 1568
John Wilson, Technical Monitor
Space Systems Division

January 1983

TABLE OF CONTENTS

THEORETICAL STUDIES OF SOLAR PUMPED LASERS

By

W.L. Harries*

SUMMARY

The work performed during the period July 1982 to January 1983 can be divided into two parts. The first part entailed finishing up the calculations on IBr, and writing up the results for publication. The final version, (see Appendix), has been submitted to Space Solar Power Review, the journal in which the previous work, "Solar Pumped Electronic to Vibrational Energy Transfer Lasers," (ref. 1) had appeared.

The second part of the work was a preliminary survey of possible new types of lasers for solar power conversion. The reason for the survey was that the efficiences of the systems considered hitherto were found to be very low. In brief, the previous investigations had first considered different absorbing (Br_2) and lasing media (CO_2, HF, HCN, H_2O) and the overall efficiency for all combinations was less than 0.5%. The above IBr laser uses the same medium for absorption and lasing and the "transfer efficiency" is largely eliminated. The final efficiency is 1.2% or less.

The new types considered were (1) liquid dye lasers, (2) vapor dye lasers, and (3) non-dissociative molecular lasers. These are discussed in the following sections.

It is tentatively concluded that liquid dye lasers would probably not be feasible. Vapor phase dye lasers offer some possibility although their overall efficiency may not be much greater than IBr. The non-dissociative molecular lasers (metallic vapor) appear promising.

LIQUID DYE LASERS AS SOLAR ENERGY CONVERTERS

An experimental investigation of liquid dye lasers is being carried out by M.D. Williams of the National Aeronautics and Space Administration.

---

*Eminent Professor, Department of Physics, Old Dominion University, Norfolk, Virginia 23508.

In general, such lasers have high gain and operate at room temperature, under giant pulse pumping. For solar pumping in the steady state a number of difficulties arise.

Lasing in organic dyes differs from one material to the other, but in general the molecules possess a pair of electrons which possess a certain freedom of motion within the molecule. The motion of this electron pair determines the electronic configuration of the molecule. The lowest electronic configuration S_0 is a singlet state (spins opposite). There are excited singlet $(S_1, S_2, ...)$ and triplet $(T_1, T_2, ...)$ states. Transitions between singlet states are "allowed" by the spectroscopic selection rules. They give rise to intense absorption and emission spectra. Transitions between different triplet states are also allowed, but singlet-triplet transitions, known as inter-system crossings, are forbidden.

The presence of molecules in one of the metastable triplet levels may be detrimental for laser action in several ways. First, the molecules stored in a triplet level are eliminated from participating in the laser cycle. Second, when some of the lowest triplet levels are populated, the material may become absorbent for the laser radiation because of triplet-triplet transitions that overlap the laser line.

It is possible to quench the triplet states, for example, by saturating the solution with oxygen, and pulses of 500 µs duration have been achieved by Schmidt (ref. 2) in air saturated rhodamine 6G solution. Commercial cw dye lasers are now available, but they have to be pumped by ultraviolet lasers. An excellent compendium on cw Dye Lasers is given by Snavely (ref. 3) and Schafer (ref. 4).

Another problem is the inducement of optical inhomogeneities (differences in reproactive index) caused by the heating and non-uniform excitation of the solution.

In conclusion, the quenching of triplet states, the presence of optical inhomogenieties, and the problem of cooling the liquid at high power levels to prevent boiling would raise severe problems for cw solar pumped liquid dye lasers.

VAPOR PHASE DYE LASERS

The use of vapors is advantageous for solar pumping, because of structural simplicity and uniformity of medium. Recently a paper by Basov et al., (ref. 5) reported experiments with vapor phase dye lasers. The results enable some tentative conclusions to be drawn on whether they would be feasible for solar pumping.

The pumping was performed with the third harmonic of a neodymium laser, at 355 nm. This wavelength lies on the low wavelength side of the solar spectrum peak which is at 500 nm, and the number of photons per unit wavelength is about half that at the peak. The absorption bandwidths of dyes in liquids are typically of order 100 nm, and if this is also true in the vapor phase, then the fraction of photons in the solar spectrum absorbed—the solar efficiency—would be somewhere in the region of 3%.

Values of efficiences of the vapor lasers were quoted, but these numbers did not include a "solar efficiency." The highest "efficiency" for a vapor phase laser was for the material POPOP, which is p-bis [2-(5-phenyloxalyl)] benzene, and was 23%. Inclusion of the solar efficiency showed gives an overall efficiency of the order of 1%.

An efficiency of over twice the above value was quoted for POPOP in liquid ether solution (a liquid dye laser). It would be unlikely that temperatures would be sufficiently low to keep the ether liquid, would be possible in a solar laser.

As steady state working would be desirable for solar lasing, the threshold pumping intensity is important. The lowest value quoted was 20 kW cm^{-2} which would correspond to the sun's radiation being concentrated 1.4×10^5 times. However, the length L of the active region of the laser was only 2.4 cm. If it is true, as in the IBr laser, that the product CL, where C is the concentration factor, is roughly constant, then C would be about 3×10^3 for L = 1m.

In conclusion, the threshold pumping intensity for such a vapor laser would be within reasonable bounds and its overall efficiency comparable to

IBr. It is noted that the experiments were performed with ether as the buffer gas at 36 atmospheres.

NON-DISSOCIATIVE DIMER LASERS

Hitherto, the types of molecular lasers considered have been those where photodissociation gave an excited atom, which then lased to the ground state. Photodissociation can also yield an excited molecule in an upper electronic state (fig. 1). The transition occurs according to the Frank Condon principle, and the molecule could return to the lower electronic level by emission of a stimulated photon. We had been aware of this possibility for some time and the suggestion of such high temperature high pressure metallic vapor lasers had been made previously (ref. 6).

A comprehensive article by Wellegehausen has reported on the development of optically pumped cw dimer lasers (ref. 7), and listed a number of experiments where lasing had occurred in Na_2, Te_2, Br_2, Li_2, K_2, and S_2, as well as in the halogens I_2 and Br_2. Here we are interested in the metallic vapor lasers. The pumping in the experiments was done by lasers, either frequency doubled Neodymium (532.5 nm) or an argon ion laser (472.7 nm). These frequencies lie near the peak of the solar spectrum. The efficiencies quoted were up to 15%, but this has to be further reduced by a "solar efficiency" for solar pumping.

If the dimer were solar pumped (fig. 2) and the temperature were high, the Frank Condon transitions would result in vibrational levels much higher than the lasing level, shown here near the upper level minimum. The high temperature has broadened the absorption bandwidth and, hence the solar efficiency. If it were possible for the molecule to cascade down in energy without any radiation transitions to ground, then there would be a "funneling" to the upper laser level. The fraction that arrives at the upper laser level depends on the probability at each level of spontaneous emission to the lower electronic level and on the probability of descending to a low rotational level by collisions or radiation. For homonuclear diatomic molecules, radiative transitions between rotational vibrations of the same electronic state are not allowed, but high pressures would enhance the collision rates.

If the "funneling" is efficient, an effect that would be considered as a "kinetic efficiency," then this type of laser would be very attractive. However, the wider the absorption band, the higher will be the initial vibrational level in the upper electronic state, and the less the probability of arriving at the upper lasing level without radiating. Also, the higher the initial vibrational level, the less will be the effective quantum efficiency. Hence, compromises will have to be made between solar kinetic and quantum efficiencies.

The possibility of lasing by solar pumping in metallic vapors such as those mentioned is being further studied and seems hopeful from the point of view of efficiency. A number of cross sections and rate constants are given in reference 7, and the possibility of kinetic modelling of such a laser is being examined.

ACKNOWLEDGMENTS

REFERENCES

1. Harries, W.L. and Wilson, J.W.: Space Solar Power Review 2, 367, 1981.

2. Schmidt, W.: Laser 2, 47, 1970.

3. Snavely, B.B.: Topics in Applied Physics. Dye Lasers, 2nd edition,
   edited by Schafer, F.P., Ch. 2, p. 120. Springer Verlag, N.Y.
4. Schafer, F.P.: Ref. 3, p. 265.

5. Basov, N.G., Logunov, O.A., Startsev, A.V., Stoilov, Yu, Yu, and Zuev,
   V.S.: J. of Molecular Structure, 79, 119, 1982.

6. Harries, W.L.: Theoretical Studies of Solar Pumped Lasers. Progress
   Report PTR-80-1 for research grant NSG-1568, Jan. 1980, Tables 1 and 2.

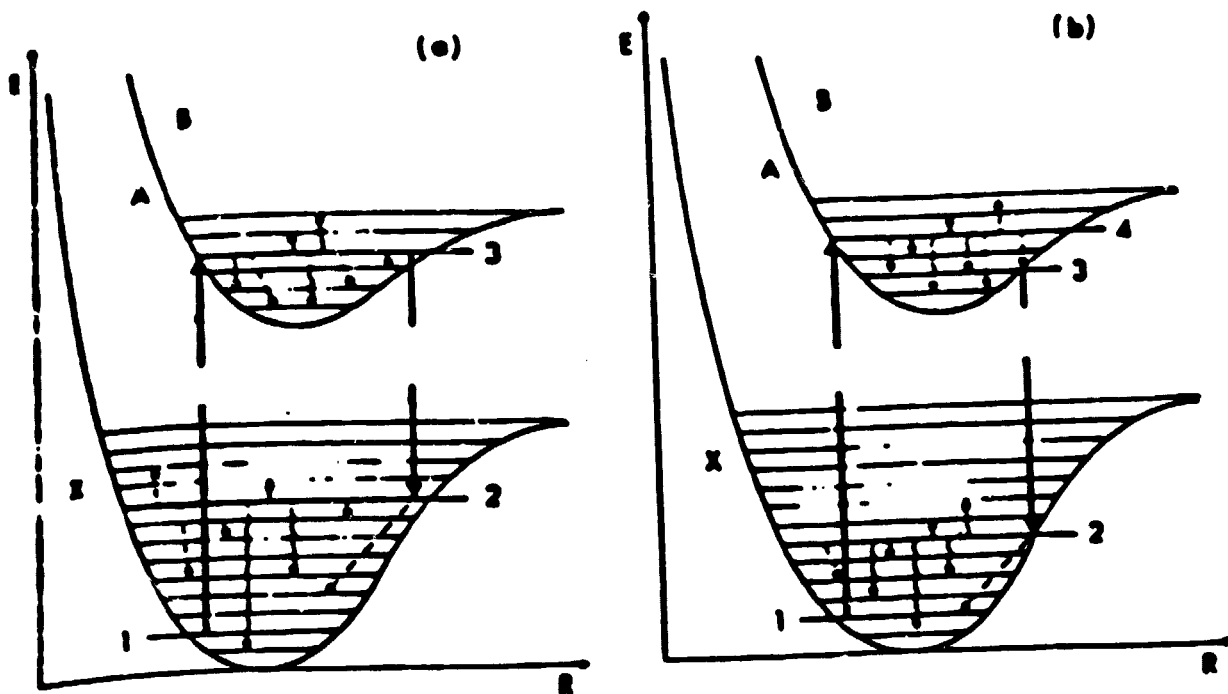7. Wellegehausen, B.: IEEE J. of Quantum Electronics, QE-15, 1108, 1979.

Figure 1. Laser cycles between bound electronic molecular states, (a) three-level cycle and (b) four-level cycle with radiative or nonradiative transitions between the levels 4 and 3.
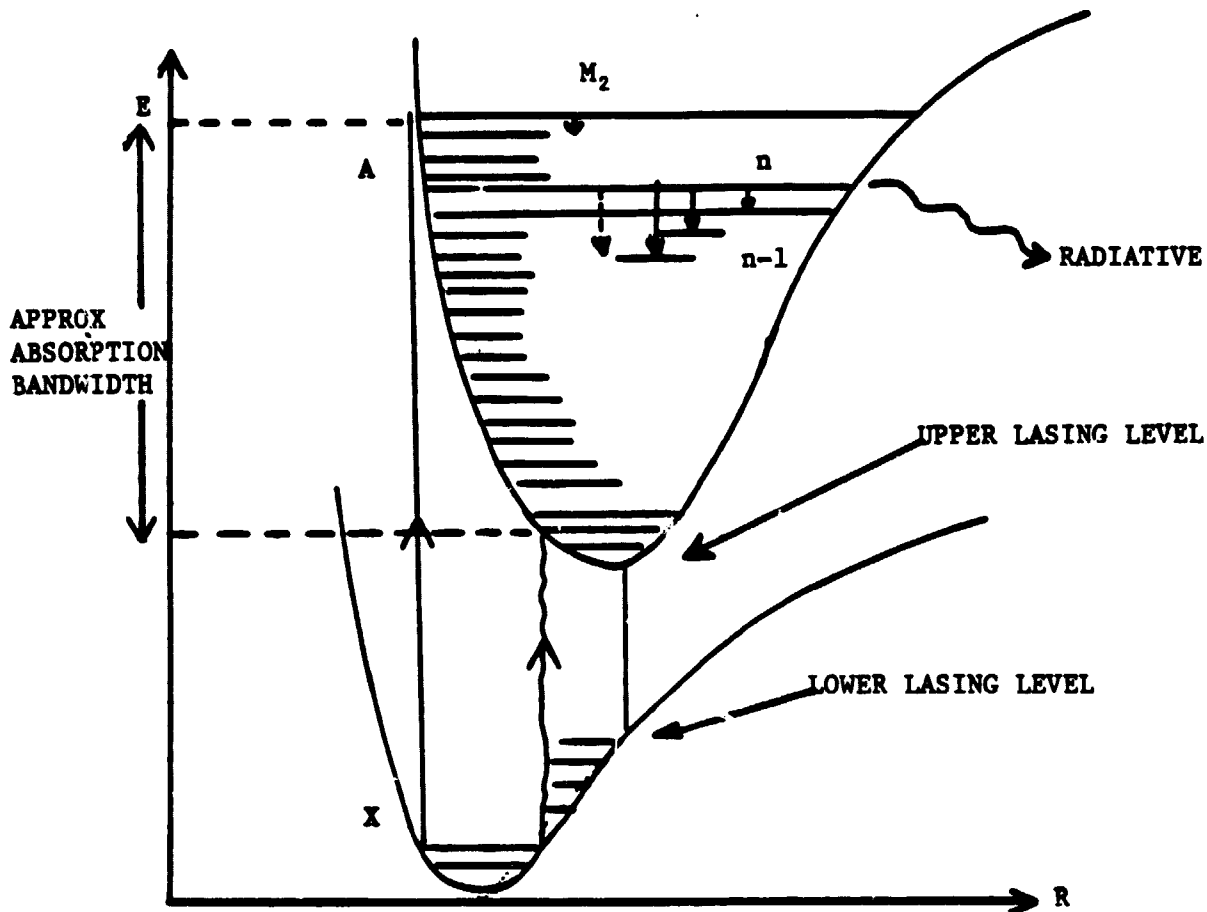
Figure 2. Energy level diagram for a solar pumped dimer molecule M_2. The
vibrational levels only are shown. A molecule raised to the nth
level of the upper electronic A state can either descend to the
(n-1), (n-2) ..., levels by collisions, (continuous arrows) and
radiation (dotted arrows) or else radiate a photon (wave arrow)
and then drop to the lower electronic X state.

8

APPENDIX

KINETIC MODELING OF AN IBr SOLAR PUMPED LASER

W.L. Harries
Old Dominion University
Norfolk, Virginia 23508

W.E. Meador
NASA/Langley Research Center
Hampton, Virginia 23665

ABSTRACT

The possibility of using an IBr laser as a solar energy converter is examined theoretically, and reasons for its choice are given. Broadband absorption results in dissociation with the formation of excited Br* atoms, some of which then lase to the ground state Br. The ground state is depopulated by three-body recombination and, more importantly, by exchange reactions which more than compensate for the high quenching in heteronuclear halogen systems. Kinetic modeling indicates lasing is possible in the pulsed mode and possibly in the steady-state with a cooled gas flow system. Temperature effects are discussed. The efficiency of the laser approaches 1.2% at optical thicknesses large enough for complete absorption of the photons.

I. INTRODUCTION

The concept of collecting solar radiation in large mirrors on orbiting space stations, and then transmitting the energy via laser beams has been considered previously (1-3). The efficiency of the system is expected to be highest if the laser could be directly pumped by the solar radiation.

The criteria for an efficient solar pumped laser are:

(a) there must be broadband absorption;

(b) peak absorption should occur near the peak of the solar spectrum;

(c) high quantum yield into a long-lived (metastable) state which serves as the upper laser level;

(d) in general, quenching of the excited state should be small, but, as will be pointed out later, this condition is alleviated if

(e) the lower level is rapidly depopulated to maintain inversion;

(f) the upper and lower levels must be sufficiently separated to yield a reasonable quantum efficiency;

10

(g) the process must be reversible; if not the components must be reconstituted by flow methods.

Gas lasers are advantageous because of uniformity of medium and because size is not a limitation. Two classes of laser can be considered: (1) where the absorbing medium is distinct from the lasant, and (2) where one material performs both functions.

The first solar pumped laser examined theoretically was type (1) above, namely a Br_2-CO_2-He mixture (2-3). The Br_2 acted as a broadband absorber, the CO_2 was the lasing medium, and the He acted as a coolant. This laser was an electronic-to-vibrational energy transfer laser, and the low "transfer efficiency" as well as absorption efficiency resulted in an overall efficiency of less than 0.13%.

Higher overall efficiency might be attained if the transfer efficiency could be eliminated, as in lasers of type (2) above. An example would be photodissociation of a molecule to yield an excited atom, which then lases to the ground state. The population of the lower level might be removed by chemical processes. High pressure working should be possible which would enable more efficient absorption.

The objectives of this paper are to study theoretically the IBr solar pumped laser as an example of class (2), to understand the essential lasing features by determining the dominating reactions, and to estimate the efficiency for power conversion. The criteria that have been listed for the selection of candidate lasants will also be assessed. In particular the question of whether steady state lasing is possible will be discussed.

As the solar radiance must be concentrated many times, and since the IBr absorption is broadband near the peak of the solar spectrum, the laser will quickly heat up and lasing inhibited (by mechanisms to be discussed),

unless cooling is provided. In the theoretical study it is therefore assumed that the lasant is maintained around room temperature, the purpose being to examine the potential for lasing under favorable operating conditions. Methods for accomplishing cooling are proposed in Section IX.

While this study was in progress, an experimental investigation of an IBr laser pumped by a xenon lamp was performed by L. Zapata (4). The objective of that experiment was to demonstrate lasing, and not necessarily to provide definitive quantitative data. Hence, only limited comparisons could be made, but the experimental results were useful in assessing the effects of excessive heating in the actual experimental environment.

II. CHOICE OF IBr

Broadband absorption is essential for high solar efficiency and there are many compounds which can be photodissociated to yield excited atoms X^*. Here only halogens are considered for X. They can be divided into three types: diatomic homonuclear molecules X_2, diatomic heteronuclear molecules YX, and complex molecules of the form RX where R is a molecular radical.

Solar pumped lasing has already been demonstrated for type RX, using a xenon arc to radiate perfluoropropyliodide C_3F_7I (5-7). Absorption occurred in the ultraviolet (230-320 nm) so that the fraction of the solar radiation absorbed (solar efficiency) was small. (Chemical recycling was also necessary for continuous working.) Types X_2 and YX on the other hand can absorb near the peak of the solar spectrum when both X and Y are halogen atoms.

The excited atoms F^*, Cl^*, Br^* and I^* have energies of about 0.1, 0.2, 0.44, and 1 eV respectively, above ground; only Br^* and I^* have values high enough to give acceptable quantum efficiencies. Lasing characteristics

12

depend on the competition between the rate of reduction of the excited species X^* by quenching and the depopulation of the lower level X by the exchange reaction $X + XY \rightarrow X_2 + Y$. Exchange reactions are possible only for heteronuclear molecules. Since the photodissociation of XY always seems to leave the lighter atom in the metastable excited state, and since the quantum efficiency increases with the atomic number of the lasing atom, it appears that IBr should be the best laser candidate of type (2). It absorbs near the solar peak with a high probability of dissociating into $I + Br^*$.

III. PHYSICAL MECHANISMS

The processes occurring in IBr are assumed to be photodissociation with the formation of excited and ground state atoms, quenching of the excited atoms, recombination and exchange reactions. The species are assumed to be eight in all, namely IBr, I, Br, I_2, Br_2, Br^*, and I^*, and photons created by spontaneous and stimulated emission. Vibrational excitations are neglected at room temperature because of very rapid relaxation. The reactions and rate constants are summarized in Table 1.

The absorption of photons results in reactions 1 through 6. The photodissociation rates S are equal to $C \, \Phi(\lambda)\Delta\lambda \, \sigma_a(\lambda) \, (N)$ where C is the number of times the solar radiation is concentrated, $\Phi(\lambda)\Delta\lambda$ is the number of photons arriving per unit area per second (8), $\sigma_a(\lambda)$ the absorption cross-section in question, and (N) the number density of absorbers. As the ratio Br^*/Br initially produced by the photodissociation of IBr is critical to attaining an inverted population, care must be taken in evaluating S_1 and S_4 in Table 1. The potential curves for the $X(^1\Sigma^+)$, $A^3\Pi_1$, and $B^3\Pi_0^+$ levels for IBr were plotted by computer on the energy diagram (Fig. 1) using data from Huber and Herzberg (9). The $B'^3\Pi^+$ is included, and is drawn in approximately. The lowest vibrational level ($v = 0$) and the Franck-Condon

13

Table 1. List of reactions.

Term		Reaction	Rate Constant	References For Rate Constants
Source	1	$h\nu$ + IBr $\rightarrow$ I + Br* $\rightarrow$ I + Br	S_{11} = C × 1.25 × 10^{15} (IBr) Br*: $-S_1$ = 0.704 S_{11} Br: $-S_4$ = 0.259 S_{11} I: $-S_7$ = 0.963 S_{11}	9, 10, 11, 13 14, 15, 16 17, 18, 19 20, 21
	2 3	$h\nu$ + I_2 $\rightarrow$ I + I* $\rightarrow$ I + I	S_{21} = C × 2.5 × 10^{15} (I_2) I*: $-S_2$ = 0.2 S_{21} I: $-S_5$ = 0.48 S_{21}	
	4 5 6	$h\nu$ + Br_2 $\rightarrow$ Br + Br* $\rightarrow$ Br + Br	S_{31} = C × 1.25 × 10^{15} (Br_2) Br*: $-S_3$ = 0.605 S_{31} Br: $-S_6$ = 1.387 S_{31}	
Quenching	7	Br* + IBr $\rightarrow$ Br + IBr	Q_1 = 1 × 10^{-12} (cm^3s^{-1})	22, 23
	8	+ I_2 $\rightarrow$ Br + I_2	Q_2 = 1.86 × 10^{-12}	22
	9	+ Br_2 $\rightarrow$ Br + Br_2	Q_3 = 4.7 × 10^{-13}	22
	10	+ I $\rightarrow$ Br + I	Q_4 = 1.8 × 10^{-11}	14
	11	+ Br $\rightarrow$ 2Br	Q_5 = 1.8 × 10^{-11} or 0	—
	12	I* + IBr $\rightarrow$ I + IBr	Q_6 = 6 × 10^{-11}	24
	13	+ I_2 $\rightarrow$ I + I_2	Q_7 = 3.5 × 10^{-11}	24, 25
	14	+ Br_2 $\rightarrow$ I + Br_2	Q_8 = 5.6 × 10^{-11}	24, 26
Recombination (2 body)	15	I_2 + Br_2 ⇌ 2IBr	K_7 → 1 × 10^{-13} K_8 → (1.6 × 10^{-16})	31
Recombination (3 body)	16	Br* + Br + IBr $\rightarrow$ Br_2 + IBr	C_1 = 4 × 10^{-32} (cm^6s^{-1})	Assumed equal to C_3
	17	Br + Br + IBr $\rightarrow$ Br_2 + IBr	C_2 = 3 × 10^{-30}	Assumed equal to C_4
	18	Br* + Br + Br_2 $\rightarrow$ $2Br_2$	C_3 = 4 × 10^{-32}	27
	19	Br + Br + Br_2 $\rightarrow$ $2Br_2$	C_4 = 3 × 10^{-30}	27
	20	Br* + I + IBr $\rightarrow$ 2IBr	C_5 = 1 × 10^{-32}	28
	21	Br + I + IBr $\rightarrow$ 2IBr	C_6 = 1 × 10^{-32}	28
	22	I* + I + IBr $\rightarrow$ I_2 + IBr	C_7 = 3 × 10^{-32}	28
	23	I* + Br + IBr $\rightarrow$ 2IBr	C_8 = 3 × 10^{-32}	28
	24	I + I + IBr $\rightarrow$ I_2 + IBr	C_9 = 3 × 10^{-30}	28
Exchange (2 body)	25	Br + IBr $\rightarrow$ I + Br_2	E_1 = 3.5 × 10^{-11} (cm^3s^{-1})	29
	26	Br + I_2 $\rightarrow$ IBr + I	E_2 = E_1 or 0	29

transitions are shown. The horizontal dashed lines B and C are based on the transitions from the lower to the upper $A^3\Pi_1$ and $B^3\Pi_0$ levels and indicate the peaks and widths of the absorption curves. The absorption cross-section for IBr as a function of wavelength has been measured (10-11), and the function can be represented by three Gaussians whose peaks are at 268, 477 and 507 nm, respectively. These are plotted on the left. The peak of Gaussian F coincides almost exactly with the line C, but the peak of the Gaussian G is displaced from B. We believe the Gaussians to be accurate as well as the asymptotes A and D.

The integral $\int_{\lambda_1}^{\lambda_2} \phi(\lambda)\sigma_a(\lambda)d\lambda$ is a measure of what fraction of absorption events are caused by transitions to the level in question and $\sigma_a(\lambda)$ is the respective Gaussian. Thus Gaussian H produces Br, but can be neglected as $\phi(\lambda)$ is small here (8). The part of Gaussian F above asymptote A produces Br*; the part below A does not produce dissociation. The $B'^3\Pi_0^+$ and $B^3\Pi_0^+$ curves cross and possibly absorption into the latter could result in Br. However, the translational energy at the crossing is sufficiently high and the nature of the crossing is such that the probability is near unity that all parts of the absorption curve above A in Figure 1 correspond to dissociation into I + Br*, as confirmed experimentally (13). The Gaussian G, corresponding to absorption into the $A^3\Pi_1$ level produces I + Br. Performing the integration of $\phi(\lambda)\sigma_a(\lambda)d\lambda$ then yielded the fractions of absorption events resulting in the production of Br*, Br, and I (Table 1). The total absorption rate for IBr was found to be $C \times 1.25 \times 10^{15}$ (IBr), where C is the number of times the solar radiation is concentrated, of which a fraction 0.704 resulted in Br*, 0.259 in Br and 0.963 in I. Similar estimates for I_2 and Br_2 are also included.

For all the initial pressures of IBr considered, it was assumed that 4% by number density of I_2 and Br_2 were present at 300 K, according to the law of mass action. Thereafter, all the densities varied with time. The absorption rate is proportional to IBr pressure for low pressures (and absorption lengths of 1 cm), until at about 50 torr essentially all the photons are absorbed.

The degeneracy factor for the upper laser level Br* is 2, while that of the lower laser level Br ($^2P_{3/2}$) is 4. The population inversion ΔN for lasing is then

$$\Delta N = Br^* - Br/2 \tag{1}$$

The degeneracy factors in this instance help to reduce the threshold for lasing.

The quenching of Br* and I* is given by reactions 7-14 in Table 1; the quenching of Br* and I* by Br* and I* was neglected as well as the quenching of Br* by Br and I* by I and Br. Computer runs in which these latter coefficients were arbitrarily assigned values equal to Q_4, instead of zero, showed no great difference in the results. The large rate coefficient for the quenching of Br* by I is due to the electronic to translational energy transfer resulting from the "crossing" of (IBr)* potential energy curves (see Fig. 1). The process has been called the inverse predissociation mechanism (14).

The two body recombination of I_2 and Br_2 (item 15) is the only reversible reaction included. At room temperature, by the law of mass action (assuming no photodissociation), the concentration of I_2 and Br_2 in IBr is 0.04. It then follows that if the forward reaction $2IBr \rightarrow I_2 + Br_2$ has a rate coefficient K_7, then the reverse coefficient K_8 is $(0.04)^2 \times K_7$.

Three-body recombinations are listed and it is seen that the reactions, involving I* and Br* are less likely than those involving I and Br because of the difficulty of getting rid of the excitation energy. Some of the values are uncertain and are based on similar reactions in I_2.

The exchange reactions that depopulate the lower laser level and make lasing possible are listed as items 25 and 26. Experimental measurements of reaction 25 have been reported by Clyne and Cruze, (27) who deduce a high rate coefficient $E_1 = 3.5 \times 10^{-11} cm^3 s^{-1}$. We have been unable to find a rate coefficient for reaction 26, but computer runs for $E_2 = 0$ and $E_2 = E_1$ did not differ greatly because the concentration of I_2 is much less than that of IBr.

IV. RATE EQUATIONS

In the following equations the terms in parenthesis represent the densities of atomic and molecular species; n is the density of photons. The quantity A is the Einstein coefficient for spontaneous emission, while Γ is the rate of stimulated emission.

The rate equations for the eight species present are:

$$\frac{d(IBr)}{dt} = -S_{11}(IBr) + C_5(I)(Br^*)(IBr) + C_6(I)(Br)(IBr)$$

$$+ C_8(I^*)(Br)(IBr) - E_1(Br)(IBr) + E_2(Br)(I_2)$$

$$+ 2K_7(I_2)(Br_2) - 2K_8 (IBr)^2 \tag{2}$$

$$\frac{d(I)}{dt} = S_7 + S_2 + 2S_5 - C_5(I)(Br^*)(IBr)$$

$$- C_6(I)(Br)(IBr) - C_7(I^*)(I)(IBr)$$

$$-2C_9(I)(I)(IBr) + E_1(Br)(IBr) + E_2(Br)(I_2) \tag{3}$$

17

$$\frac{d(I_2)}{dt} = -S_{21}(I_2) + C_7(I*)(I)(IBr) + C_9(I)(I)(IBr) - E_2(Br)(I_2) \quad (4)$$

$$\frac{d(Br_2)}{dt} = -S_{31}(Br_2) + C_1(Br*)(Br)(IBr) + C_2(Br)(Br)(IBr)$$

$$+ C_3(Br*)(Br)(Br_2) + C_4(Br)(Br)(Br_2)$$

$$+ E_1(Br)(IBr) - K_7(I_2)(Br_2) + K_8(IBr)^2 \quad (5)$$

$$\frac{d(Br*)}{dt} = S_1 + S_3 - C_1(Br*)(Br)(IBr) - C_3(Br*)(Br)(Br_2)$$

$$- C_5(Br*)(I)(IBr) - Q_1(Br*)(IBr) - Q_2(Br*)(I_2)$$

$$- Q_3(Br*)(Br_2) - Q_4(Br*)(I) - Q_5(Br*)(Br)$$

$$- A\ Br* - \Gamma \quad (6)$$

$$\frac{d(Br)}{dt} = S_3 + S_4 + 2S_6$$

$$+ Q_1(Br*)(IBr) + Q_2(Br*)(I_2) + Q_3(Br*)(Br_2)$$

$$+ Q_4(Br*)(I) + Q_5(Br*)(Br)$$

$$- C_1(Br*)(Br)(IBr) - 2C_2(Br)(Br)(IBr)$$

$$- C_3(Br*)(Br)(Br_2) - 2C_4(Br)(Br)(Br_2)$$

$$- C_6(Br)(I)(IBr) - C_8(Br)(I*)(IBr)$$

$$- E_1(Br)(IBr) - E_2(Br)(I_2) + A\ Br* + \Gamma \quad (7)$$

$$\frac{d(I*)}{dt} = S_2 - Q_6(I*)(I_2) - Q_7(I*)(IBr) - Q_8(I*)(Br_2)$$

$$- C_7(I*)(I)(IBr) - C_8(I*)(Br)(IBr) \quad (8)$$

$$\frac{dn}{dt} = \Gamma + GA(Br*) - \frac{n}{\tau_c} \tag{9}$$

The quantity G in equation (9) is the geometrical factor $2r_b^2/L^2$, where r_b is the radius of the laser beam and L the length of the laser; for isotropic spontaneous emission only this fraction of photons is confined within the laser cavity. The last term represents the loss through the end mirrors of reflectivities r_1 and r_2, and τ_c is the lifetime of an average stimulated emission photon travelling parallel to the axis; $\tau_c = -L/c \ln(r_1 r_2)$, where c is the velocity of light. Here $\tau_c = 5 \times 10^{-8}$ s. The quantity Γ, the stimulated emission rate, is equal to $n \sigma_e c \Delta N$ where σ_e is the stimulated emission cross-section. Then $\sigma_e = \lambda_e^4 A/4\pi^2 \Delta\lambda_e$, where λ_e is the emitted wavelength, A (≈ 1) is the Einstein coefficient for spontaneous emission from the upper laser level, and $\Delta\lambda_e$ is the emission bandwidth. With $\Delta\lambda_e$ taken as the bandwidth for Doppler broadening at 300° K, then $\sigma_e = 1.6 \times 10^{-17}$ cm^2.

Equations (2) through (9) were solved by computer, and are compared with the experimental results of Zapata in Figs. 2a and b. In the experiment, the light intensity from the xenon lamp was measured with a photo-detector, and varied approximately as $\sin^2 \dfrac{2\pi t}{2 \times 10^{-4}}$, where t is in seconds. The theoretical source terms included this function.

IV. COMPARISON WITH EXPERIMENT

The idealized model differed from the experiment in a number of ways. The theory assumed absorption occurred one-dimensionally in a thickness d. Experimentally the pumping source was a xenon lamp placed parallel to the laser tube. Its light was focussed onto the laser tube axis by a reflecting

cylinder of elliptical cross-section. The illumination increased towards the axis, but as the source was distributed and the reflector was not perfectly elliptical, the maximum value of the pumping photon flux density was uncertain. The pumping density was equated to C times the solar radiance. The values of the equivalent C in the experiments were probably between 2,000 and 40,000 for the various runs. There were also differences in the spectral distribution of the xenon lamp and the solar spectrum assumed.

Fig. 2 compares the measured light output from a 1-m long IBr laser pumped by a xenon discharge lamp powered from a capacitor bank, with the computer solution of equations (2) through (9). The IBr pressure was 3 torr and C was about 5,000 in the experiment, which are the values assumed in the calculations.

The overall shape of the experimental and calculated laser output are similar. Both start about the same time, and consist of a sharp spike followed by a tail. The ratio of spike to tail is higher in the calculated version, and the oscillations in the theoretical wave shape are not evident in the experiment. Estimates of the time constant of the InAs photodetector circuit showed it was high enough to reduce the high frequency components of the signal.

The duration of the experimental pulse for this and all other runs was always shorter than the calculated values by a factor of about two. We believe this was due to the lasant being heated near the axis. Rough calculations of the IBr gas temperature, assuming C = 5,000, indicated a temperature rise of several hundred K in 50 μs. The temperature rise would cause dissociation of IBr and deplete the lasant. This view is consistent with an experimental measurement of IBr density on the laser axis during a

pulse, which showed a drop of about 50%, a value too high to have been caused by photodissociation (it would require $C > 10^5$). High temperatures could also increase the ratio of reverse to forward rates of the exchange reactions, thus tending to neutralize the mechanisms necessary to depopulate the lower laser level (30). Also, the quenching reaction Br* + I → Br + I is enhanced in the heated gas because of the greater number of I atoms. The calculations assumed no heating.

On changing the pressure p both experiment and theory showed the output laser pulse duration was roughly independent of p for pumping pulses of 200 μs duration. Experimentally the output light signal amplitude increased with p up to about 20 torr, where it reached a maximum and then decreased; as p increased, absorption in the outer layers decreased the pump power on axis. The theory showed the amplitude proportional to p because constant pumping energy density was assumed throughout the gas.

Both experiment and theory showed that increasing C increased the laser amplitude proportionally.

There was also agreement between the measured and calculated output power of the laser. In an experiment with a tube length of 1m and 2.22 cm radius, and an output mirror of 95% transmittance, the measured output was approximately 2 kW for an IBr pressure of 4 torr, with $C \approx 10^4$ (/).

The calculated peak output power P is

$$P = \frac{1}{2} \, c \, n \, h\nu \, \tau \, \pi \, r^2 \tag{10}$$

Our results showed $n = 1.2 \times 10^{12}$ cm^{-3} for $C = 1 \times 10^4$, corresponding to 1.7 kW which is in reasonable agreement.

V. INTERPRETATION

By varying the parameters in the program one at a time, it was established that the dominant mechanisms were quenching of Br^* by IBr and I and the exchange reaction $Br + IBr = I + Br_2$. In particular, the program indicated lasing would not occur if the exchange reaction was removed. Three-body recombinations made little difference to the shape of the light output for pumping pulses of 200 μs duration. Fortunately the rate coefficients most accurately known turned out to be dominant ones. However, for computer runs of longer duration pulses, it was found essential to include all the terms.

Evidently the exchange reactions can overcome quenching, and high quenching cross-sections per se may not be a valid selection criterion for rejecting otherwise promising gases.

VI. THRESHOLD CONDITION

The threshold condition is $r_1 r_2 \exp(2\alpha L) = 1$, where $r_1 r_2$ are the reflectivities of the laser mirrors, $\alpha = \sigma_e \Delta N$ is the gain per unit length, and L is the length of the laser (30). The threshold condition is contained in equation (9), and occurs when $\Gamma > n/\tau_c - GA(Br^*) = n/\tau_c$. The two relations are equivalent as can be seen from the definition of τ_c and require $\Delta N \cdot L > \ln(1/r_1 r_2)/2\sigma_e = $ constant. As $\Delta N \propto C$ it follows that the threshold value for C is proportional to $1/L$. Computer runs were performed for successively lower values of C for $L = 400, 100,$ and 25 cm, and the threshold values of C estimated. The values are compared with experimental results in Figure 3. The absolute values of the latter were difficult to estimate as the pumping light was focused on a cylinder, but both theory and experiment show $C \propto L^{-1}$. Thus C can be reduced by increasing L.

VII. EFFICIENCY OF THE LASER

Estimates of the efficiency can be obtained from solutions of the rate equations. For a laser of length L, collecting width w and of 1 cm absorption depth, the total solar power into the laser is 0.14 CLw watts. The power output is 0.5 c $nh\nu\tau w$. If the transmission factor τ is 0.05, the efficiency is $\eta = 3.93 \times 10^{-10}$ n/CL, where n is the photon density it in cm^{-3}, and L is in cm. Computer runs at various values of L, C and gas pressures were made and the maximum n obtained to give η (fig. 4). For $L > 5$ m η is roughly independent of L and C, and at 5 torr $\eta = 5 \times 10^{-4}$. At these low pressures $\eta \propto p$ and it can be seen that higher pressures increase η, provided overheating can be avoided.

An understanding of why the efficiency is low can be obtained if the overall efficiency is considered to be the product of four efficiences (3): $\eta = \eta_s \eta_a \eta_k \eta_Q$. Here η_s, the solar efficiency depends on the absorption bandwidth of the total solar radiance, and its value for IBr is 0.12. The absorption efficiency η_a depends on the IBr gas pressure and depth of absorption d; for low pressures $\eta_a = \sigma_a(IBr)d = 10^{-2}$ pd where p is the pressure in torr, d the depth in cm. The expression is valid up to $pd = 50$; for higher pd most of the photons are absorbed and $\eta_a \to 1$. The kinetic efficiency η_k depends on the number of absorption events producing Br* and also on the competition between stimulated emission and quenching. Approximately 0.7 Br* atoms are produced for every absorbed photon (Table I). The fraction of Br* atoms which yield a stimulated photon can be obtained by examining equation 6, and comparing the value of Γ with the rest of the loss processes, as all eight variables vs time were known. The ratio Γ/(all loss processes) was 0.82 when η was a maximum, the major competitors with Γ being quenching by IBr and I. The quantum efficiency

$\eta_a = 0.44$ eV/2.5 eV $= 0.18$. Hence for pd $<$ 50 torr cm $\eta = 6 \times 10^{-4}$ at 5 torr, $d = 1$ cm, agreeing with 5×10^{-4} in Figure 4. With pd $>$ 50 torr-cm, $\eta_a \rightarrow 1$ and the maximum efficiency would be about $1 \cdot 2 \times 10^{-2}$.

Pulsed working would further reduce the efficiency because of the duty cycle, unless there was adequate storage of energy when the laser was not emitting.

VIII. POSSIBILITY OF CONTINUOUS LASING

The computer runs showed that IBr was depleted, while the quenchers I_2, Br_2 and I grew with time. For 200 µs pumping pulses, the photon density n had a maximum value just prior to the peak input.

The input light pulse was then assumed to be proportional to $\sin^2 2\pi t/10^{-4}$ up to 50 µs and thereafter to be constant. For $p = 3$ torr the calculations indicated a pulse of 350 µs, and for $p = 13$ torr the duration was of order 10 ms with C $= 5000$. Plots of the other variables indicated a gradual depletion of IBr and a growth of I. The long time scale suggests that a gas flow system would be feasible for steady-state working provided the gas temperature was kept within limits.

IX. TEMPERATURE EFFECTS

As the absorbed photons have an average energy of several eV, and as the heat conduction of IBr is low, very high temperatures can occur. If the pressure p of IBr is greater than 50 torr in a vessel 1 cm deep then the temperature of the lasing gas can be roughly estimated assuming all the photon energy is deposited in the gas; if p $\ll$ 50 torr then roughly a fraction 10^{-2} p is deposited. The heat produced travels an average distance x to the walls of the containing vessel by gaseous conduction. The walls are assumed at a temperature T_w and are thermally connected to a radiator into space. Above about 1,000 K, the gas would also act as a blackbody

24

radiator. Estimates show that if $x = 0.5$ cm, then for $C = 2,000$ and $p = 5$ torr the gas temperature would be of order 1,000 K.

If the pressure is increased (a requirement for high absorption efficiency) still higher temperatures are possible, as heat conduction in gases is independent of pressure. Cooling can be enhanced by reducing x by inserting fingers in the gas, or by admitting a noble gas with a high heat conductivity and a low quenching cross-section. Assuming perfect conduction from the walls to a radiator the same size as the collector, then the radiator temperature would be somewhat less than 300 K.

High temperatures can have large effects on quenching, recombination and dissociation rates, and on exchange reactions.

To our knowledge experimental data on the effect of temperature on the quenching of Br^* by IBr or I_2 are not available. The possible analogous case of quenching of I^* by I_2 was reported by Kartazaef et al. (31), whose measurements showed the quenching rates at 1,000 K were 20 times lower than at 300 K. If a similar dependence occurred for the quenching coefficient of Br^* by IBr or I_2, the high temperatures would prove advantageous in this respect.

Turner and Rapagnani (26) have reported measurements of the recombination rates for $I + I + I_2 \rightarrow 2I_2$ where $k = 1.1 \times 10^{-10} T^{-5.884}$. The coefficient is 1,000 times smaller at 1,000 K than at 300 K and is analogous to C_6 used above where I recombined with Br and the third body was IBr.

High temperatures cause thermal dissociation of IBr with the formation of I, Br, and Br_2, which have large cross-sections for the quenching of Br^*. The depletion of the lower level by exchange reactions would also be reduced as the increase in I would enhance the reverse exchange reaction. On

balance then, heating would seem to be very detrimental to IBr solar laser operation.

X. CONCLUSIONS

The time varying solutions of the species rate equations (2) through (9) show that inversion is possible near the start of a pumping pulse, but continuous lasing may not occur. The reason is that early in the pulse the Br created from Br* by quenching and stimulated emission is sufficiently removed by exchange reactions to maintain inversion. Eventually, however, the IBr decreases and the Br density increases to cut off the lasing.

The dominating mechanisms are the source terms, quenching by IBr and I, two body exchange reactions and stimulated emission. With 200 μs pumping pulses the behavior of the light output can be represented using only these reactions. However, if long pulses are to be simulated, then all the reactions must be included. Our computer results showed that for 3 torr of IBr, steady depletion occurred and the pulse lasted for about 350 μs with C = 5,000, L = 1m. At 13 torr the pulses were many tens of ms for the same conditions.

The exchange reactions can overcome the effect of high quenching cross-sections, and high quenching need not necessarily indicate that a material is unsuitable for solar pumped lasing.

Heating will reduce quenching. It will also cause dissociation and depletion of IBr with the formation of I, I_2, Br and Br_2 all of which quench Br*. The exchange reaction rates will be reduced causing the population inversion to disappear, thus killing the laser.

If the path length L is small, requiring the solar concentration C to be high for threshold to be reached, then the pressure has to be kept low to prevent heating (<<50 torr). The overall efficiency η is then 10^{-4} p

(torr) or 0.1% at 10 torr. Such a 10 kW laser would require a collector of 85 × 85 m^2. If L is large, so that overheating does not occur, and p is high enough to absorb all the photons, then η could reach 1.2% - a 10 kW laser collector would be 30 × 30 m^2. The above efficiencies can be compared to the calculated efficiencies of a Br_2-CO_2-He laser and a C_3F_7I laser, each of which was around 0.1%.

The effective length L can be increased by multiple passes in a flat "box type" laser. If L = 10 m, then lasing should be possible with C = 300. The temperature rise would then be 770° even if p = 50 torr, with A_1/x = 8, T_w = 300 and no admixture of a cooling gas. The receiving area of the laser would be 400/300 = 1.4 m^2 and an effective length L of 10 m could be achieved in about 8 passes.

The possibility of steady state working seems feasible if a continuous flow system is used.

ACKNOWLEDGEMENTS

REFERENCES

1. Coneybear, J.F.: The Use of Lasers for the Transmission of Power. Radiation Energy Conversion in Space ed. K.H. Billman. Program in Astronautics and Aeronautics, 61, 279, 1979.

2. Gyordiets, B.F., Gudzenko, L.I., and Pachenko, V. Ya: Pis' ma Zh Eksp, Teor. Fiz. 26, 163, 1977.

3. Harries, W.L. and Wilson, J.W.: Space Solar Power Review. 2, 367, 1981.

4. Zapata, L.: Private communication.

5. Lee, J.H. and Weaver, W.R.: Appl. Phys. Lett. 39, 137, 1981.

6. Weaver, W.R. and Lee, J.H.: Proceedings of the 16th Intersociety Energy Conversion Engineering Conference, Atlanta, Georgia, Aug. 9-14, 1981 p. 84.

7. Wilson, J.W. and Lee J.H.: Proc. Virginia Acad. of Sci. 31, 34, 1980.

8. Carter, J.R. and Tada, H.Y.: Solar Cell Radiation Handbook. Jet Propulsion Laboratory, California Institute of Technology, Report No. 21945-6001, RV OU 1973, Table 2.1, p. 2-2.

9. Huber, K.P., and Herzberg, G.: Molecular Spectra and Molecular Structure-Constants of Diatomic Molecules. Van Nostrand, 1978.

10. Seery, D.J. and Britton, D.: J. Phys. Chem. 68, 2263, 1964.

11. Passchier, A.A., Christian, J.D. and Gregory, N.W.: J. Phys. Chem. 71, 1937, 1967.

12. DeVries, M.S., Van Teen N.J.A., Baller, T. and De Vries, A.E.: Chem. Phys. Lett. 75, 27, 1980.

13. Petersen, A.B., Smith, W.M.: Chem. Physics 30, 407, 1978.

14. Faist, M.B. and Bernstein, R.B.: J. Chem. Physics, 64, 2971, 1976.

15. Hohla, K. and Kompa, K.L.: Handbook of Chemical Lasers, R.W.F. Lyon and J.F. Bolt editors, John Wiley (NY) 1976, ch. 12.

16. Burde, D.H., McFarlane, R.A., and Wiesenfeld, J.R.: Phys. Rev. Aio, 1917, 1974.

17. Tellinghuisen, J.: J. Chem. Phys. 58, 2821, 1973.

18. Wellegehausen, B., Stephan, K.H. Friede, D., and Welling, H.: Optics Communications 23, 157, 1977.

19. Beverly, R.E. and Wong, M.C.: Optics Communications 20, 23, 1977.

20. Petersen, A.B., Smith, W.M.: Chemical Physics 30, 407, 1978.

21. Hofmann, H. and Leone, S.R.: Chem. Phys. 54, 314, 1978.

22. Gordon, E.B., Nadkhin, A.I., Sothichenko, S.A., and Boriev, I.A.: Chem. Phys. Lett. 86, 2, 1982.

23. Hofmann, H. and Leone, S.R.: J. Chem. Phys. 69, 641, 1978.

24. Burde, D.H. and McFarlane, R.A.: J. Chem. Phys. 64, 1850, 1976.

25. Appleman, E.H., and Clyne, M.A.A.: J. Chem. Soc. Farad Trans. 2, 72, 191, 1976.

26. These numbers are based on similar reactions in I_2: Turner, C. and Rapagnani, N.L. Laser Fusion Program Semi-annual Report UCRL-50021-13-1 Lawrence Livemore Laboratory UCID-16935 Jan.-Jun. 1973.

27. The values of C_5-C_9 are based on similar reactions, $I + I + I_2$ and $I^* + I + I_2$ _ Hohla, K. and Kompa, K.L.: The Photochemical Iodine Laser. Ch. 12 of Handbook of Chemical Lasers, Ed. by R.W.F. Lyons and J.F. Bolt. Wilder and Sons, N.Y., 1976.

28. Clyne, M.A.A., and Cruze, H.W.: J. Chem. Soc. Farad Trans. 2, 68, 1377, 1972.

29. Lengyel, B.A.: Lasers. 2nd Ed. John Wiley, 1971, p. 61.

30. This suggestion was made by L. Zapata.

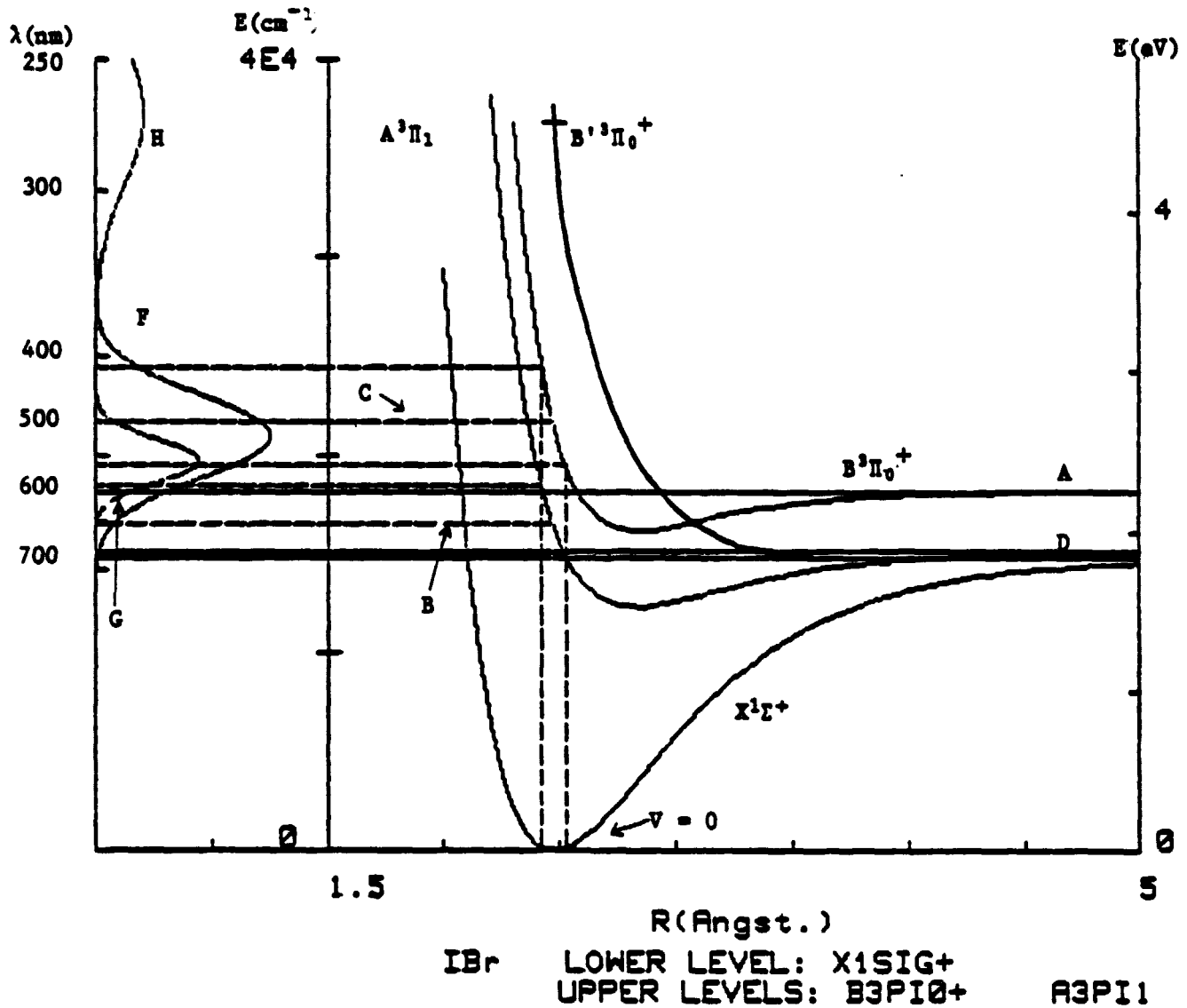31. Kartazaef, V.A., Penkin, N.P., and Tolmachev, Yu. A.: Sov. J. Quantum Electronics, Vol. 7, 1977, p. 608.

Figure 1. Energy level diagram for IBr. The potential curves $X(^1\Sigma^+)$, $A^3\Pi_1$, $B^3\Pi_0^+$ are Morse functions generated from data of Huber and Herzberg. The repulsive curve $B'^3\Pi_0^+$ is approximate. The Gaussian absorption curves are plotted from data of Seery and Britton.
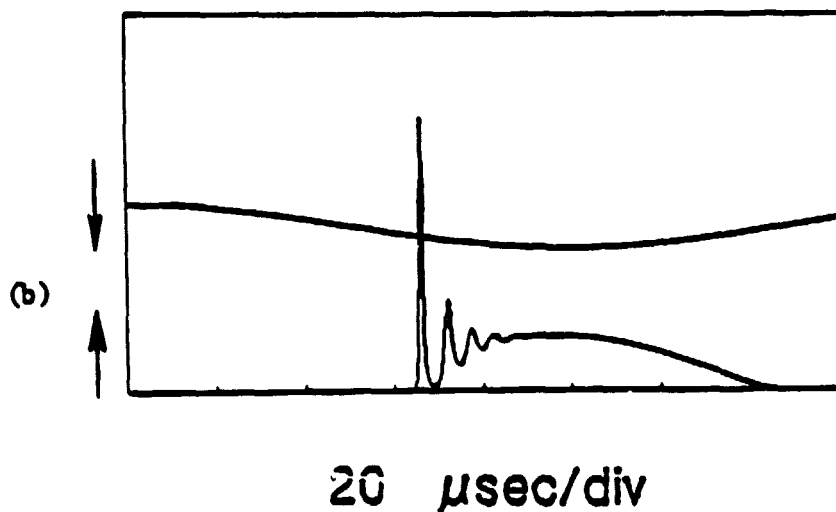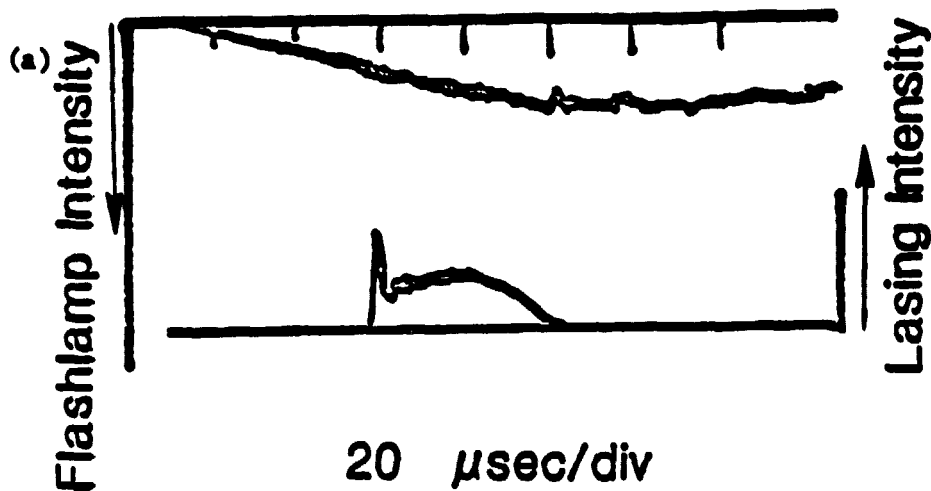
31

Figure 2. Comparison of (a) measured laser light output vs. time compared
with (b) calculated values. The pressure of IBr was 3 t.rr, with
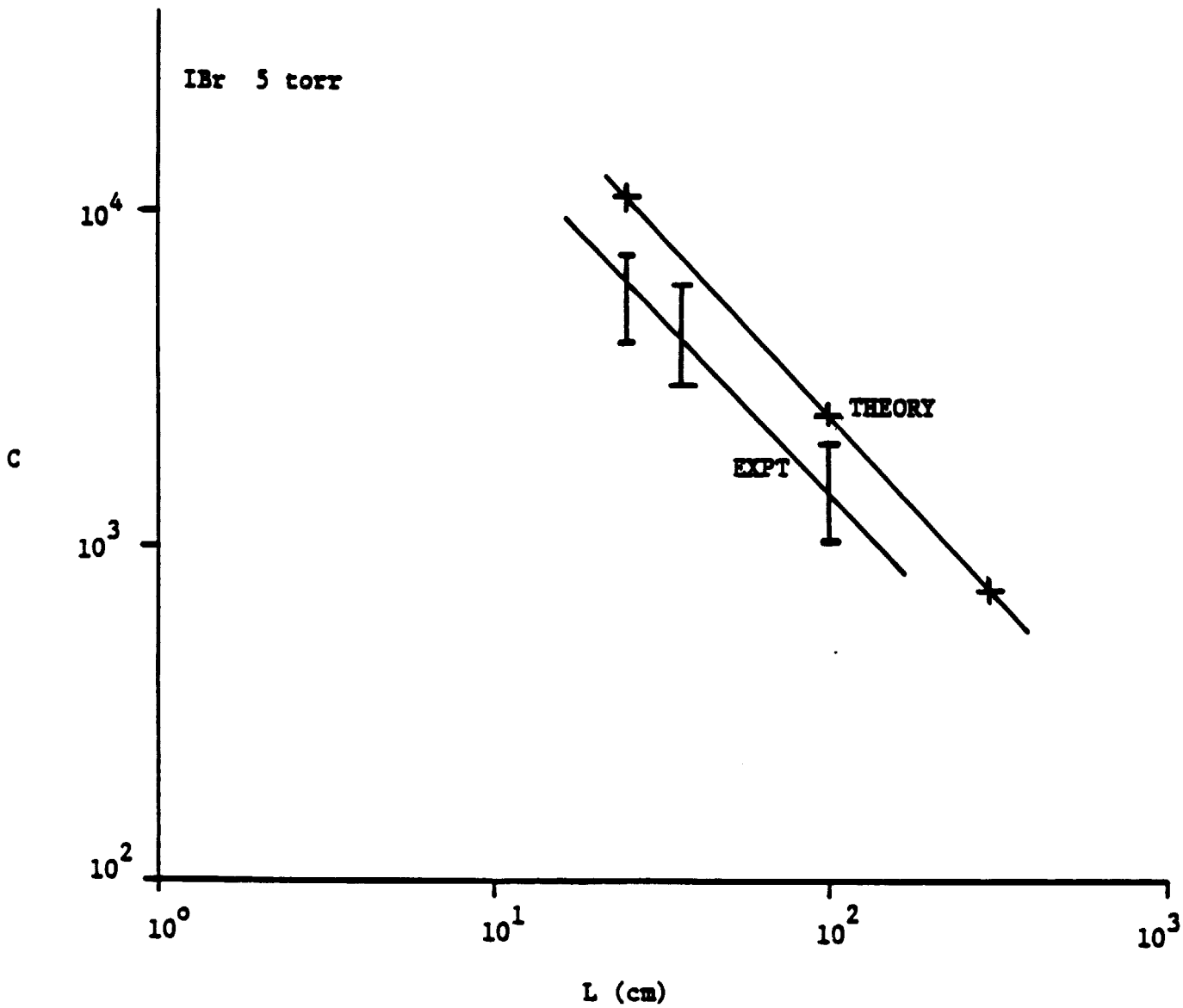4% Br_2, I_2. In the calculations C = 5,000. The pumping light
intensity is inverted.

IBr 5 torr

C

L (cm)

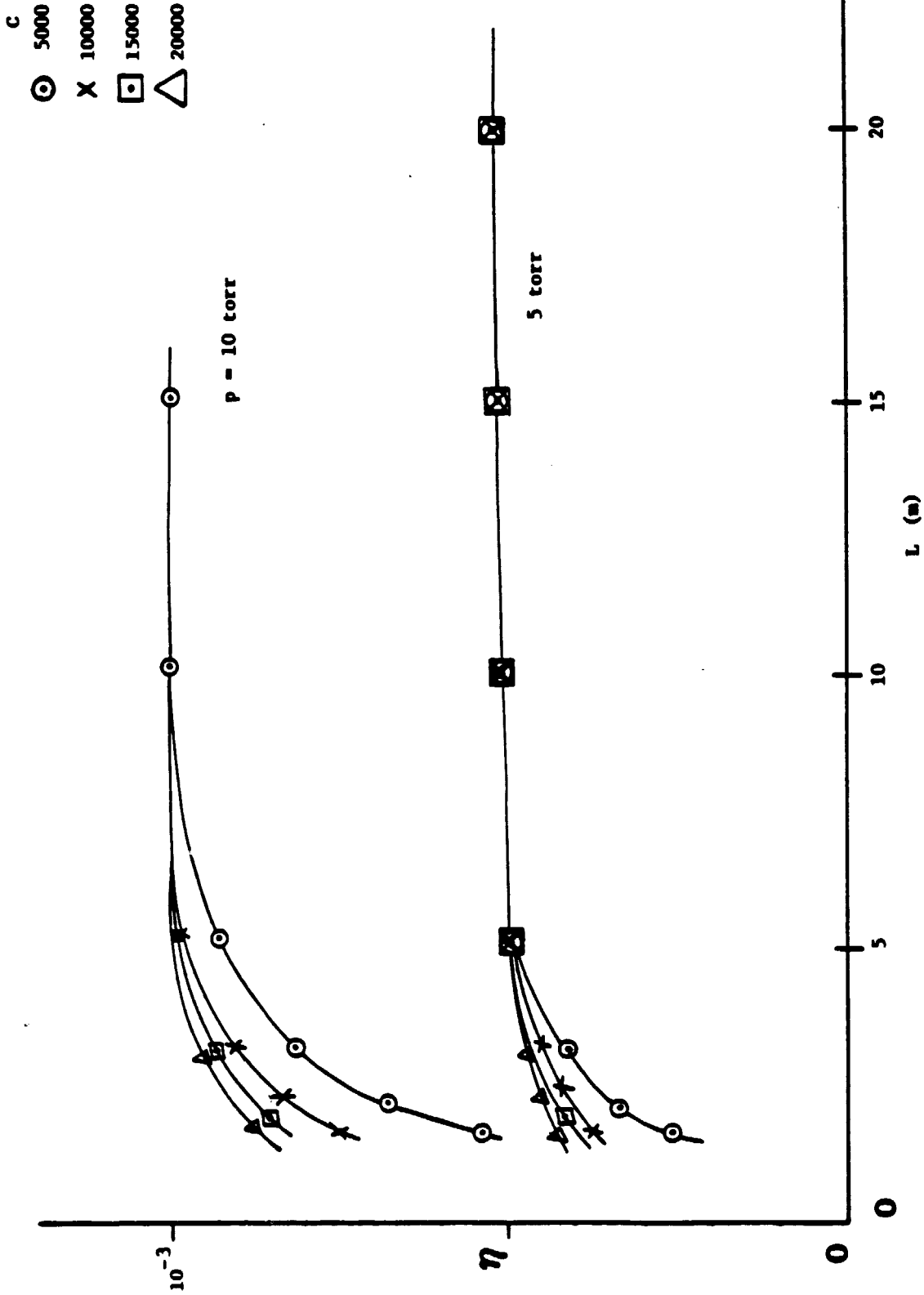Figure 3. Plot of lowest C for lasing vs. laser length L.

Figure 4. Efficiency of IBr solar pumped laser plotted vs length L at different pressures, and concentration factors C. The reflectivities are $r_1 = 1$, $r_2 = 0.95$, respectively.

34